

EVLA Memo #176

High-sensitivity bandpass calibration: Combining observations in time

Claire Murray (UW Madison), W. M. Goss (NRAO), Snežana Stanimirović (UW Madison)

January 28, 2014

Abstract

We demonstrate that bandpass calibration observations can be combined in time in order to reduce noise in bandpass solutions. Multiple bandpass sources can be used, between observations spaced in time by up to one week and possibly longer. This strategy is very useful for filler-project observing, as it allows for reduced calibration overhead time per observing file without compromising sensitivity in the final calibration solution.

1 Introduction

We are conducting a high sensitivity survey of HI absorption lines, called 21-SPONGE (“21-cm SPectral line Observations of Neutral Gas with the (E)VLA”), in order to detect signatures broad, shallow absorption lines with peak optical depth $\tau \sim 0.001$. We aim to reach rms noise levels in optical depth of $\Delta\tau \sim 5 \times 10^{-4}$, and therefore we require high sensitivity and stable baselines in order to reliably detect these lines. To achieve this we require very sensitive bandpass solutions, and typically allocate up to 40 percent of every observation to bandpass calibration overhead.

In order to minimize noise levels in bandpass solutions, we have experimented with averaging bandpass observations acquired at different times. While investigating this time stability, we found that the bandpass solutions contain a sinusoidal “ripple” with a period of 59 kHz caused by the application of finite impulse response filters prior to correlation (see EVLA Memo 171[1]). After subtracting the ripple, we find the noise in a combined bandpass solution improves by nearly the theoretically expected amount from the ideal radiometer equation, i.e. by $1/\sqrt{\Delta t}$ for a factor of Δt increased integration time.

2 Method

Our observations involve standard L-band configurations, each with one dual polarization IF of 0.5 MHz bandwidth covered by 256 channels (at 1.95 kHz per channel). We use two configurations, one centered at 1.421908 GHz (1.5 MHz, or about 316 km/s, higher than the HI rest frequency, called “high”) and one at 1.418908 GHz (1.5 MHz lower, called “low”) in order to perform bandpass calibration for HI line observations. By using this frequency switching technique, we avoid typically strong emission and absorption lines that would contaminate the profiles of the bandpass calibrators at the HI rest frequency, as well as avoid increased system temperature from HI emission and possible

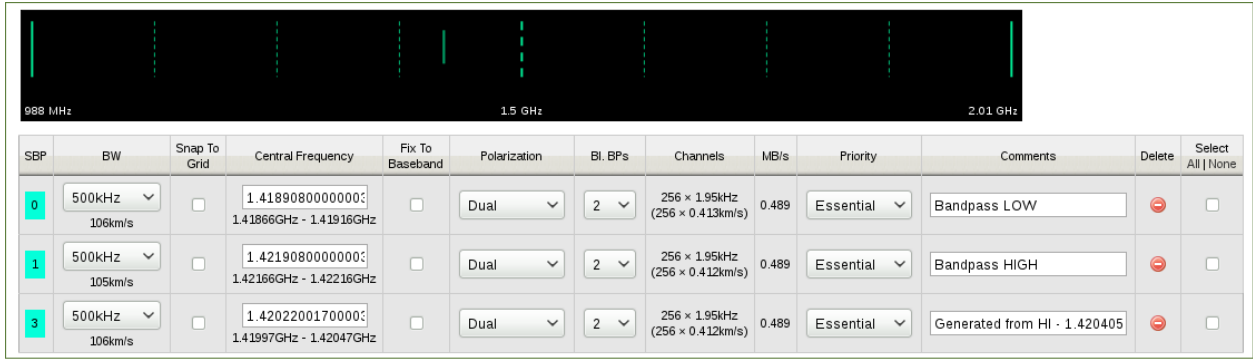


Figure 1: Instrument configuration display from the OPT. We perform bandpass calibration by frequency switching. The two 0.5 MHz bandpass calibration subbands, “HIGH” and “LOW”, are offset from the central HI observation subband by 1.5 MHz ($\sim 316 \text{ km s}^{-1}$) in order to avoid HI absorption lines from the strong bandpass calibrators, resolved emission in the close array configurations, and increased system temperature noise from strong HI emission.

resolved emission in the closest array configurations. Figure 1 displays the instrument configuration from the OPT.

We favor the strong calibrators, 3C286, 3C147 and 3C48 for bandpass calibration. As a filler project, we operate with short (~ 1 hour) scheduling blocks so that we must maximize efficiency (and minimize slew time). If a target is bright enough ($S_{1.4\text{GHz}} \geq 6 \text{ Jy}$), we use it as its own bandpass calibrator. This is possible given our small bandwidth (0.5 MHz). For a 6 Jy source, in order to reach rms noise levels of $\sim 5 \times 10^{-4}$, we need at least 2 hours of total integration time per bandpass calibrator.

We perform all data reduction in AIPS. After flagging and initial bandpass calibration of the “high” and “low” frequency offset bandpass observations using BPASS, we combine the “high” and “low” data and re-compute the bandpass solution with BPASS. To test the stability of the bandpass solutions in time, we combine observations conducted on separate days and recompute a bandpass solution. We then export the final bandpass tables using POSSM for further analysis outside of AIPS.

To compare noise levels in the BP solutions from the original observation and the combined observations, we first model and remove the 59 kHz ripple present in all solutions[1]. The ripple is caused by finite impulse response filters applied prior to correlation which shape the bandpass. The ripple is stable in time (the period, amplitude and phase are constant between all examined solutions acquired over the past 3 years of observations[1]) so that we are able to model and remove it after combining the observations. Figure 2 shows an example of the modeling process. A zoom-in onto a bandpass solution from one observation of 3C147 (33 min integration) is shown in the top left panel, with the ripple model overlaid in red. The top right panel displays the residuals following the removal the ripple model, from which the noise in the bandpass solution is computed. The bottom panels are the same, after adding an additional observation of 3C147 from 4 days later (for a total of $33+30=63$ min integration).

3 Results

We expect the noise in the bandpass solution to decline according to the factor of increase in integration time (Δt) given by the ideal radiometer equation, or by $1/\sqrt{\Delta t}$. For example, from

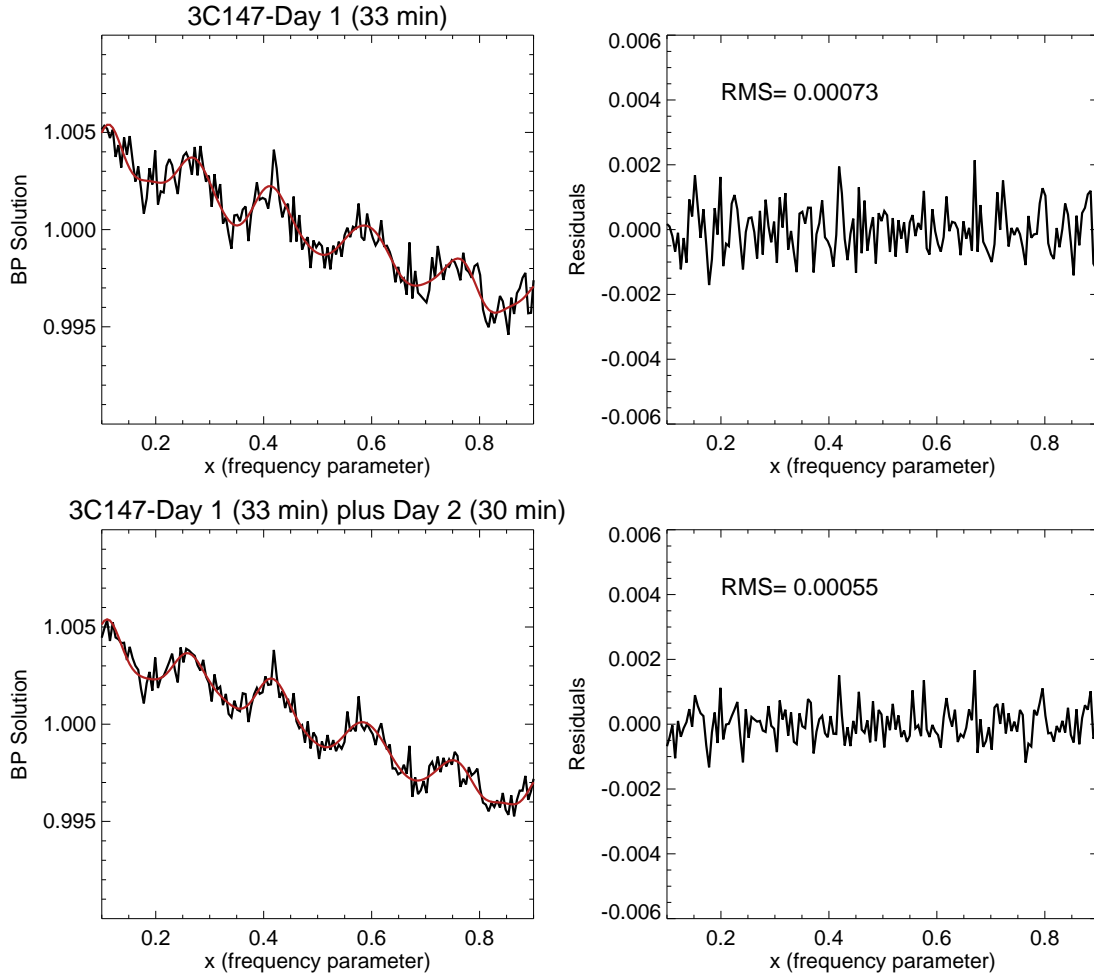


Figure 2: An example of the process. We fit the bandpass solutions (left) for the presence of a 59 kHz ripple, remove this model (shown in red) to produce the panels on the right, from which we measure the rms noise in the solution. The top panels are from a single observation, and the bottom panels are the results of adding an observation 4 days later.

Figure 2, for an increase in integration time of $\Delta t = 63/33 = 1.9$, we expect an improvement in noise by a factor of $1/\sqrt{\Delta t} = 1.38$. The improvement in noise is $0.00073/0.00055 = 1.33$.

In Figure 3 we show the rms noise in the bandpass solution (computed after removing the ripple) as a function of Δt for several different observations (symbols). The solid lines denote the expected decline in noise level, and the amount of time between observations is quoted next to each measurement. It is clear that the noise declines at nearly theoretical expectations in all cases.

In this process, we are able to combine observations of different sources. In Figure 3, the green triangles are from a trial combining observations of the sources 3C410 ($S_{1.4\text{GHz}} = 10\text{ Jy}$) and 3C454.3 ($S_{1.4\text{GHz}} = 11\text{ Jy}$) as bandpass calibrators. The other three cases are combinations of observations of the same bandpass calibrators, 3C147 ($S_{1.4\text{GHz}} = 23\text{ Jy}$) and 3C286 ($S_{1.4\text{GHz}} = 15\text{ Jy}$) between several days. These examples represent a common trend in our results.

In recent observations, we experimented with including additional 0.5 MHz subbands spaced $\pm 1.5, 3$ and 4.5 MHz from the HI line. We found that combining these subbands does not significantly

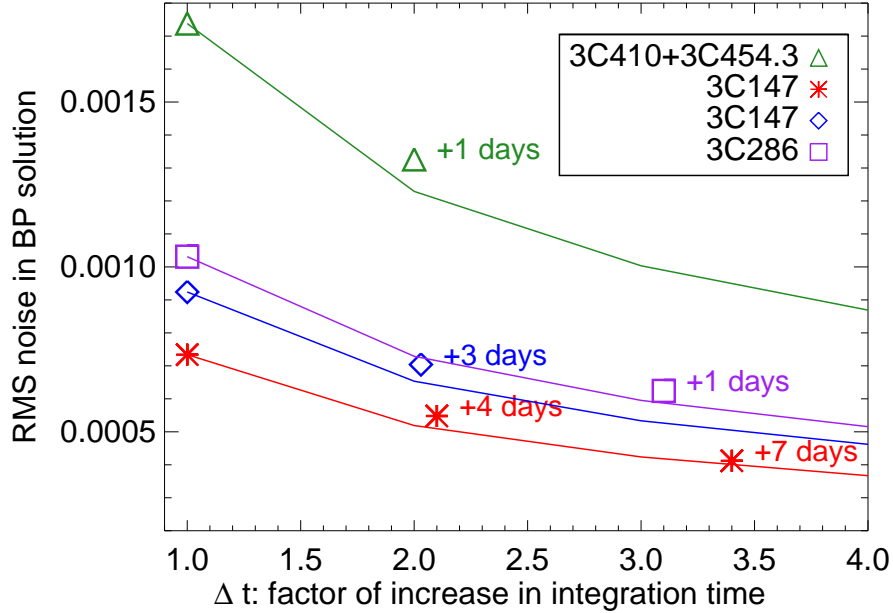


Figure 3: The improvement in rms noise in a bandpass solution (y-axis) by combining observations in time, thereby increasing the total integration time (x-axis). Symbols denote measurements, and solid lines display the theoretical prediction (e.g. noise decrease by factor of $1/\sqrt{\Delta t}$).

improve the noise in the bandpass solution, due to the change in bandpass slope with increasing subband separation.

4 Conclusions

We have shown that it is possible to combine frequency-switched bandpass observations over narrow bandwidths in order to improve noise levels in the bandpass solutions. Multiple sources can be combined to this effect, and the noise level improves at nearly the theoretically expected level (i.e. by $1/\sqrt{\Delta t}$ for a factor of Δt increase in total integration time). This has great implications for minimizing calibration overhead time for filler-project observations, which must rely on short observations without compromising sensitivity.

References

- [1] Murray, C. E., Goss, W. M., & Stanimirović, S., 2013, EVLA Memo 171. www.aoc.nrao.edu/evla/geninfo/memoseries/evlamemo171.pdf